Small-Animal PET of Tumors with ^{64}Cu-Labeled RGD-Bombesin Heterodimer

Zhaofei Liu[1,2], Zi-Bo Li[1], Qizhen Cao[1], Shuanglong Liu[1], Fan Wang[2], and Xiaoyuan Chen[1]

[1]Molecular Imaging Program at Stanford, Department of Radiology, Biophysics Program, and Bio-X Program, Stanford University School of Medicine, Stanford, California; and [2]Medical Isotopes Research Center, Peking University, Beijing, China

The overexpression of gastrin-releasing peptide receptor (GRPR) in various tumor types suggests that GRPR is an attractive target for cancer imaging and therapy with radiolabeled bombesin analogs. We recently reported the ability of ^{18}F-labeled RGD-bombesin heterodimer to be used for dual integrin $\alpha_v\beta_3$– and GRPR-targeted imaging. To further investigate the synergistic effect of the dual-receptor targeting of peptide heterodimers, we evaluated ^{64}Cu-labeled RGD-bombesin for PET imaging of tumors. **Methods:** RGD-bombesin was coupled with 1,4,7,10-tetraazacyclododecane-*N*, *N*′, *N*′′, *N*′′′-tetraacetic acid (DOTA) and 1,4,7-triazacyclononane-1,4,7-triacetic acid (NOTA), and the conjugates were labeled with ^{64}Cu. The in vitro and in vivo characteristics of ^{64}Cu-NOTA-RGD-bombesin were compared with those of ^{64}Cu-NOTA-RGD, ^{64}Cu-NOTA-bombesin, and ^{64}Cu-DOTA-RGD-bombesin. **Results:** ^{64}Cu-NOTA-RGD-bombesin and ^{64}Cu-DOTA-RGD-bombesin had comparable dual integrin $\alpha_v\beta_3$– and GRPR-binding affinities in vitro, both of which were slightly lower than RGD for integrin binding and bombesin for GRPR binding. ^{64}Cu-NOTA-RGD-bombesin possessed significantly higher tumor uptake than did ^{64}Cu-NOTA-RGD, ^{64}Cu-NOTA-bombesin, the mixture of ^{64}Cu-NOTA-RGD and ^{64}Cu-NOTA-bombesin, or ^{64}Cu-DOTA-RGD-bombesin in PC-3 prostate cancer. ^{64}Cu-NOTA-RGD-bombesin also showed improved in vivo kinetics such as lower liver and intestinal activity accumulation than did the bombesin tracers. ^{64}Cu-NOTA-RGD-bombesin also outperformed ^{64}Cu-NOTA-RGD in a 4T1 murine mammary carcinoma model that expresses integrin on tumor vasculature but no GRPR in tumor tissue, which had no uptake of ^{64}Cu-NOTA-bombesin. **Conclusion:** Compared with other tracers, ^{64}Cu-NOTA-RGD-bombesin showed favorable in vivo kinetics and enhanced tumor uptake, which warrants its further investigation for targeting tumors that express integrin or GRPR or that coexpress integrin and GRPR for imaging and therapeutic applications. The synergistic effect of RGD-bombesin heterodimers observed in this study also encourages further investigations of novel heterodimers recognizing other cell surface receptors for tumor targeting.

Received Dec. 31, 2008; revision accepted Mar. 31, 2009.
For correspondence or reprints contact either of the following:
Xiaoyuan Chen, Department of Radiology, Stanford University School of Medicine, 1201 Welch Rd., P095, Stanford, CA 94305-5484.
E-mail:shawchen@stanford.edu
Fan Wang, Medical Isotopes Research Center, Peking University, 38 Xueyuan Rd., Beijing, 100191, China.
E-mail: wangfan@bjmu.edu.cn

Key Words: RGD-BBN heterodimer; bombesin; positron emission tomography (PET); gastrin-releasing peptide receptor (GRPR); integrin $\alpha_v\beta_3$; ^{64}Cu

J Nucl Med 2009; 50:1168–1177
DOI: 10.2967/jnumed.108.061739

Bombesin is a 14-amino-acid peptide that was originally purified from amphibian skin (*1*). The bombesin receptors, in particular the gastrin-releasing peptide receptor (GRPR) subtype, were found to be overexpressed in several types of human cancer, such as lung cancer, colon cancer, gastric cancer, pancreatic cancer, breast cancer, and prostate cancer (*2,3*). The relatively low expression of GRPR in normal tissues and increased expression in the cancer tissues has validated GRPR as a target for cancer detection and treatment. In recent years, a series of bombesin and analogs was labeled with various isotopes such as ^{99m}Tc, ^{111}In, ^{64}Cu, ^{177}Lu, ^{18}F, or ^{68}Ga and investigated for GRPR-positive tumor-targeted imaging and therapy in both animal models and human trials (*4–8*).

Recently, we synthesized a bombesin-RGD heterodimer from GRPR-specific bombesin (bombesin(7–14)) and integrin $\alpha_v\beta_3$-specific RGD (c(RGDyK)) through a glutamate linker, which is a mixture of RGD on the Glu side-chain γ-position (Glu-bombesin-RGD) and bombesin on the Glu side-chain γ-position (Glu-RGD-bombesin) (*9*). The ^{18}F-labeled RGD-bombesin heterodimer showed significantly improved tumor-targeting efficacy and pharmacokinetics, compared with ^{18}F-labeled RGD and bombesin monomers. In our follow-up study (*10*), we synthesized Glu-RGD-bombesin and inserted a long-chain polyethylene glycol (PEG_3), 11-amino-3,6,9-trioxaundecanoic acid spacer onto the glutamate α-amino group of Glu-RGD-bombesin to increase the overall hydrophilicity and to alleviate steric hindrance, thereby increasing the ^{18}F labeling yield. The resulting ^{18}F-labeled RGD-bombesin heterodimer exhibited excellent in vivo kinetics and dual GRPR- and integrin $\alpha_v\beta_3$ receptor–targeting properties in PC-3 tumor-bearing nude mice (*10*).

In the PC-3 prostate cancer xenograft, the receptor density of GRPR is much higher than that of integrin $\alpha_v\beta_3$ (2.7×10^6 GRPRs per cell vs. 2.76×10^3 integrins per cell) (*8,10,11*). In our previous studies (*9,10*), we found that excess doses of bombesin were more efficient at inhibiting

uptake of radiolabeled RGD-bombesin in PC-3 tumors than was RGD, suggesting that the bombesin motif in the RGD-bombesin heterodimer contributes more than the RGD motif to high tumor uptake of the tracer in GRPR-positive PC-3 tumors. In this study, we labeled the RGD-bombesin heterodimer with ^{64}Cu and compared the ^{64}Cu-labeled RGD-bombesin with the 2 monomeric counterparts. ^{64}Cu (half-life, 12.7 h; β^+, 17.8%; $E_{\beta+max}$, 656 keV; β^-, 38.4%; $E_{\beta-max}$, 573 keV) (*12*) is well suited for the in vitro and in vivo characterization of peptide probes, especially at late time points (e.g., 24 h). Moreover, the conjugates used for ^{64}Cu labeling can be applied to other copper isotopes and transition metal isotopes for the purposes of radionuclide imaging and internal radionuclide therapy (*13*).

1,4,7,10-Tetraazacyclododecane-*N*, *N*′, *N*′′, *N*′′′-tetraacetic acid (DOTA) is one of the most investigated bifunctional chelators for ^{64}Cu labeling. However, the relatively low thermodynamic and kinetic stability of ^{64}Cu-DOTA in vivo has been well documented (*14–17*). The instability of the ^{64}Cu-DOTA conjugates would result in demetallation and subsequent accumulation in nontarget tissues such as liver (*15*). Prasanphanich et al. recently reported ^{64}Cu-labeled bombesin analogs using 1,4,7-triazacyclononane-1,4,7-triacetic acid (NOTA) as a chelator. The results suggested high in vivo kinetic stability of ^{64}Cu-NOTA-bombesin vectors with little or no dissociation of ^{64}Cu from NOTA (*15*).

The purposes of the current study were severalfold: first, we wanted to investigate the potential advantages of ^{64}Cu-labeled NOTA-RGD-bombesin heterodimer over the monomeric counterparts NOTA-RGD and NOTA-bombesin for imaging GRPR-positive tumors (e.g., PC-3); second, we wanted to compare the in vitro and in vivo characteristics of ^{64}Cu-labeled RGD-bombesin heterodimer using NOTA as a chelator with those using DOTA as a chelator; and third, we also wanted to test the feasibility of using ^{64}Cu-NOTA-RGD-bombesin to image tumors that express integrin but not GRPR (e.g., 4T1 murine mammary carcinoma).

MATERIALS AND METHODS

General

All commercially obtained chemicals were of analytic grade and used without further purification. DOTA and *S*-2-(4-isothiocyanatobenzyl)-NOTA were purchased from Macrocyclics. 1-Ethyl-3-[3-(dimethylamino)-propyl] carbodiimide, *N*-hydroxysulfonosuccinimide, and Chelex 100 resin (50–100 mesh) were purchased from Sigma-Aldrich. Water and all buffers were passed through a Chelex 100 column before use in radiolabeling procedures to ensure that the aqueous buffer was free of heavy metals. The peptides Aca-bombesin(7–14) and c(RGDyK) were synthesized by Peptides International. RGD-bombesin heterodimer was synthesized from Aca-bombesin(7–14) and c(RGDyK) as we previously described (*10*). ^{125}I-[Tyr^4]bombesin (74 TBq/mmol (2,000 Ci/mmol)) was purchased from GE Healthcare, Na^{125}I was purchased from Perkin-Elmer, and ^{64}Cu was obtained from the University of Wisconsin. The reversed-phase high-performance liquid chromatography (HPLC) system was the same as previously reported (*9,10*). For the purification of DOTA and NOTA conjugated peptides, a Vydac protein and peptide column (218TP510; 5 μm, 250 × 10 mm) was used with a flow rate of 5 mL/min. For analytic HPLC and radiolabeling purification, a Vydac 218TP54 column (5 μm, 250 × 4.6 mm) was used with a flow rate of 1 mL/min. The mobile phase was changed from 95% solvent A (0.1% trifluoroacetic acid in water) and 5% solvent B (0.1% trifluoroacetic acid in acetonitrile) (0–2 min) to 35% solvent A and 65% solvent B at 32 min. The ultraviolet absorbance was monitored at 218 nm, and the identification of the peptides was confirmed through the ultraviolet spectrum acquired using a photodiode array detector. The radioactivity was detected by a model 105S single-channel radiation detector (Carroll and Ramsey Associates).

Synthesis of NOTA and DOTA Conjugates

NOTA-c(RGDyK) (NOTA-RGD), NOTA-Aca-bombesin(7–14) (NOTA-bombesin) and NOTA-RGD-bombesin conjugates were prepared as we previously described (*18*). In brief, a solution of 2 μmol of peptide (RGD, bombesin, or RGD-bombesin) was mixed with 6 μmol of *S*-2-(4-isothiocyanatobenzyl)-NOTA in 0.1N $NaHCO_3$ solution (pH 9.0). After 5 h of stirring at room temperature, the NOTA conjugates were isolated by semipreparative HPLC. NOTA-RGD was obtained in 61% yield with more than 95% purity on analytic HPLC (retention time [R_t], 13.4 min). Matrix-assisted laser desorption/ionization time-of-light mass spectrometry (MALDI-TOF-MS): mass-to-charge ratio (m/z), 1,070.4 for $[MH]^+$ ($C_{47}H_{68}N_{13}O_{14}S$, calculated molecular weight, 1,070.5). NOTA-bombesin was obtained in 72% yield with more than 95% purity on analytic HPLC (R_t, 22.05 min). MALDI-TOF-MS: m/z, 1,504.0 for $[MH]^+$ ($C_{69}H_{102}N_{18}O_{16}S_2$, calculated molecular weight, 1,503.8). NOTA-RGD-bombesin was obtained in 52% yield with more than 95% purity on analytic HPLC (R_t, 20.72 min). MALDI-TOF-MS: m/z, 2,235.3 for $[MH]^+$ ($C_{101}H_{148}N_{28}O_{26}S_2$, calculated molecular weight, 2,234.6). RGD-bombesin was also conjugated with DOTA using our previously described method (*19*). Briefly, DOTA was activated by 1-ethyl-3-[3-(dimethylamino)-propyl] carbodiimide and *N*-hydroxysulfonosuccinimide for 30 min with a molar ratio of 10:5:4 for DOTA:1-ethyl-3-[3-(dimethylamino)-propyl] carbodiimide:*N*-hydroxysulfonosuccinimide. The DOTA-OSSu (6 μmol, calculated on the basis of *N*-hydroxysulfonosuccinimide) was added to RGD-bombesin (2 μmol) in 0.1N $NaHCO_3$ solution (pH 9.0). After being stirred at 4°C overnight, the DOTA conjugate was isolated by semipreparative HPLC. DOTA-RGD-bombesin was obtained in 60% yield with more than 95% HPLC purity (R_t, 20.63 min). MALDI-TOF-MS: m/z, 2,171.2 for $[MH]^+$ ($C_{97}H_{148}N_{28}O_{27}S$, calculated molecular weight, 2,170.4).

^{64}Cu Labeling

About 5–10 nmol of NOTA-RGD, NOTA-bombesin, NOTA-RGD-bombesin, or DOTA-RGD-bombesin dissolved in NaOAc buffer were labeled with ^{64}Cu at 42°C for 1 h for DOTA conjugates and at room temperature for 15 min for NOTA conjugates. The labeled peptides were then purified by analytic HPLC. The radioactive peak containing the desired product was collected and rotary-evaporated to remove the solvent. The products were then formulated in phosphate-buffered saline and passed through a 0.22-μm Millipore filter into a sterile multidose vial for in vitro and in vivo experiments.

Cell Lines and Animal Models

The PC-3 human prostate carcinoma cells were grown in F-12K medium, and the 4T1 murine breast cancer cells were grown in

RMPI 1640 medium. Both cell lines were cultured in medium supplemented with 10% (v/v) fetal bovine serum at 37°C with 5% CO_2. The PC-3 tumor model was generated by subcutaneous injection of 5×10^6 tumor cells into the right front flank of male athymic nude mice (Harlan). The 4T1 tumor model was generated by subcutaneous injection of 5×10^6 tumor cells into the left front flank of female normal BALB/c mice (Harlan). The mice were used for small-animal PET studies when the tumor volume reached approximately 100–300 mm^3 (~3–4 wk after inoculation for PC-3 and ~1–2 wk for 4T1). All animal procedures were performed according to a protocol approved by the Stanford University Institutional Animal Care and Use Committee.

Cell-Binding Assay

The in vitro dual-receptor binding affinity of NOTA-RGD-bombesin and DOTA-RGD-bombesin was determined by a cell-binding assay as we previously described (*10,20*). ^{125}I-c(RGDyK) was generated by labeling c(RGDyK) with Na^{125}I using our previously reported method (*21*). ^{125}I-c(RGDyK) and ^{125}I-[Tyr^4] bombesin were used as radioligands for integrin $\alpha_v\beta_3$ and GRPR, respectively.

Cell Uptake and Efflux Studies

The cell uptake and efflux studies were performed as we previously described (*9,10,22*). The cell uptake was expressed as the percentage added dose after decay correction. Efflux values at different time points were calculated by subtracting retention from 0-min retention and normalized by dividing it by the total counts at 0 min. Experiments were performed twice with triplicate wells.

Small-Animal PET

PET and image analysis were performed using a microPET R4 rodent model scanner (Siemens Medical Solutions) as previously reported (*9,19*). Under isoflurane anesthesia, each PC-3 tumor mouse received an injection via the tail vein of approximately 5.5 MBq (150 μCi) of ^{64}Cu-NOTA-RGD, ^{64}Cu-NOTA-bombesin, ^{64}Cu-NOTA-RGD-bombesin, ^{64}Cu-NOTA-RGD (75 μCi) plus ^{64}Cu-NOTA-bombesin (75 μCi), or ^{64}Cu-DOTA-RGD-bombesin. Five-minute static PET images were acquired at 30 min, 1 h, and 4 h after injection of each tracer (n = 4/group), and 10-min static PET images were acquired at 20 h. The images were reconstructed using a 2-dimensional ordered-subsets expectation maximum algorithm without attenuation or scatter correction. Under isoflurane anesthesia, each 4T1 tumor mouse received an injection via the tail vein of 3.7 MBq (100 μCi) of ^{64}Cu-NOTA-RGD, ^{64}Cu-NOTA-bombesin, or ^{64}Cu-NOTA-RGD-bombesin. Five-minute static PET images were then acquired at 2 h after injection (n = 3/group). A series of blocking studies was also performed as we previously described (*9,10*) to validate the in vivo dual-receptor binding affinity of ^{64}Cu-NOTA-RGD-bombesin in PC-3 tumor-bearing nude mice at 1 h after injection of about 5.5 MBq (150 μCi) of tracer (n = 3/group). For each small-animal PET scan, regions of interest were drawn over each tumor, over normal tissue, and over major organs using vendor software (ASI Pro, version 5.2.4.0) on decay-corrected whole-body coronal images. The maximum radioactivity concentration (accumulation) within a tumor or an organ was obtained from the mean pixel values within the multiple-region-of-interest volume, which were converted to MBq/mL/min using a conversion factor. Assuming a tissue density of 1 g/mL, the regions of interest were converted to MBq/g/min and then divided by the administered activity to obtain an imaging region-of-interest–derived percentage injected dose (%ID)/g.

Biodistribution Studies

Normal BALB/c mice received an injection via the tail vein of 370 kBq (10 μCi) of ^{64}Cu-NOTA-RGD-bombesin to evaluate the distribution of the tracer. The blocking experiments were also performed by coinjection of ^{64}Cu-NOTA-RGD-bombesin with a saturating dose of c(RGDyK) (10 mg/kg of mouse body weight), bombesin (15 mg/kg), or RGD (10 mg/kg) plus bombesin (15 mg/kg). All mice were sacrificed at 1 h after injection of the tracer. Blood, tumor, and major organs and tissues were collected and wet-weighed. Stomach and intestines were cleaned of their contents in this experiment. The radioactivity in the tissue was measured using a γ-counter (Packard). The results were presented as percentage injected dose per gram of tissue (%ID/g). Values were expressed as mean ± SD (n = 4/group).

Statistical Analysis

Quantitative data were expressed as mean ± SD. Means were compared using 1-way ANOVA and the Student t test. P values less than 0.05 were considered statistically significant.

RESULTS

Chemistry and Radiochemistry

The NOTA conjugates of RGD, bombesin, and RGD-bombesin and the DOTA conjugate of RGD-bombesin were analyzed by HPLC and mass spectroscopy to confirm the identity of the products. The structures of DOTA-RGD-bombesin and NOTA-RGD-bombesin are shown in Figure 1. On the analytic HPLC, no significant difference in retention time was observed between ^{64}Cu-labeled tracers and the unlabeled NOTA and DOTA conjugates. NOTA-RGD-bombesin was more easily labeled with ^{64}Cu than was DOTA-RGD-bombesin as determined by the labeling condition studies (Supplemental Fig. 1A; supplemental materials are available online only at http://jnm.snmjournals.org). For in vitro and in vivo studies, the specific activity of the ^{64}Cu tracers after labeling and purification was typically about 7.4–14.8 MBq/nmol (~0.2–0.4 Ci/μmol), with radiochemical purity greater than 98% as determined by analytic radio-HPLC.

Cell-Binding Assay

The integrin $\alpha_v\beta_3$ receptor-binding affinities of DOTA-RGD-bombesin and NOTA-RGD-bombesin were compared with c(RGDyK) by conducting a competitive binding assay on U87MG cells using ^{125}I-c(RGDyK) as the radioligand. The inhibitory concentrations of 50% for DOTA-RGD-bombesin, NOTA-RGD-bombesin, and c(RGDyK) were 21.55 ± 2.19 nM, 16.15 ± 2.77 nM, and 10.84 ± 2.55 nM, respectively (Supplemental Fig. 1B). The binding affinities of DOTA-RGD-bombesin, NOTA-RGD-bombesin, and Aca-bombesin(7–14) for GRPR were evaluated on GRPR-positive PC-3 cells using ^{125}I-[Tyr^4]bombesin as the radioligand. The inhibitory concentrations of 50% were determined to be 85.79 ± 2.08 nM for DOTA-RGD-bombesin, 92.75 ± 3.53 nM for NOTA-RGD-bombesin, and 71.57 ± 3.06 nM for Aca-bombesin(7–14) on PC-3 cells (Supplemental Fig. 1C).

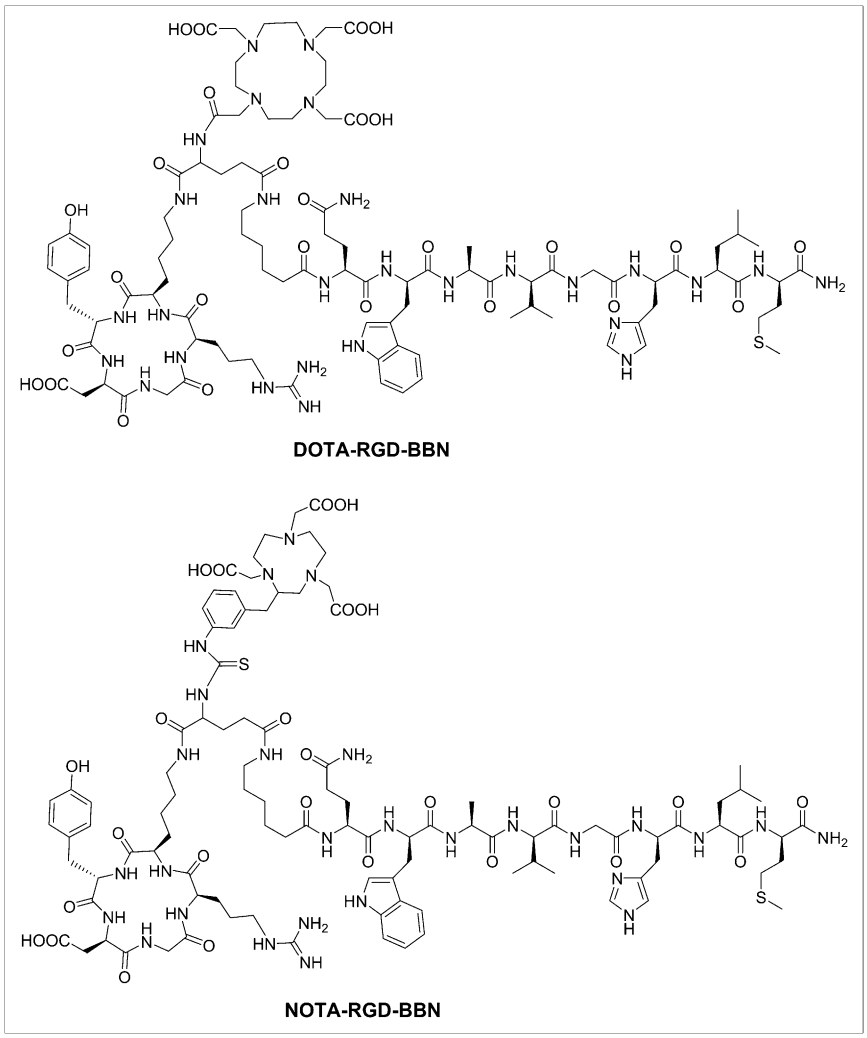

FIGURE 1. Chemical structures of DOTA-RGD-bombesin and NOTA-RGD-bombesin. RGD-bombesin is a heterodimer of cyclic RGD peptide c(RGDyK) and Aca-bombesin(7–14) through a glutamate linker, with RGD attached to α-carboxylate and bombesin attached to γ-carboxylate. BBN = bombesin.

Cell Uptake and Efflux Studies

^{64}Cu-NOTA-bombesin showed a rapid and high uptake in the PC-3 tumor cells, whereas ^{64}Cu-NOTA-RGD had low cell uptake (Fig. 2A). The cell uptake values of ^{64}Cu-NOTA-RGD-bombesin and ^{64}Cu-DOTA-RGD-bombesin were between those of ^{64}Cu-NOTA-bombesin and ^{64}Cu-NOTA-RGD. The amplified cell uptake comparison of ^{64}Cu-NOTA-RGD-bombesin and ^{64}Cu-DOTA-RGD-bombesin is shown in Supplemental Figure 1D. Cell uptake of ^{64}Cu-NOTA-RGD-bombesin was slightly more rapid than that of ^{64}Cu-DOTA-RGD-bombesin during the first 30 min of incubation and then reached a similar value at 60 min. At 120 min, the cell uptake value was 3.70% ± 0.02% added dose for ^{64}Cu-DOTA-RGD-bombesin and 2.94% ± 0.51% added dose for ^{64}Cu-NOTA-RGD-bombesin. The cell efflux ratio of ^{64}Cu-NOTA-RGD was higher than that of ^{64}Cu-NOTA-bombesin or ^{64}Cu-NOTA-RGD-bombesin (Fig. 2B). Because ^{64}Cu-NOTA-RGD did not seem to be internalized into the PC-3 cells, the cell efflux reflected mainly dissociation of ^{64}Cu-NOTA-RGD from the tumor cells, as the RGD monomer has relatively low affinity for integrin $\alpha_v\beta_3$. Compared with ^{64}Cu-NOTA-bombesin, ^{64}Cu-NOTA-RGD-bombesin showed a relatively low efflux ratio with time. After 2 h, the efflux of both ^{64}Cu-NOTA-RGD-bombesin and ^{64}Cu-NOTA-bombesin reached a

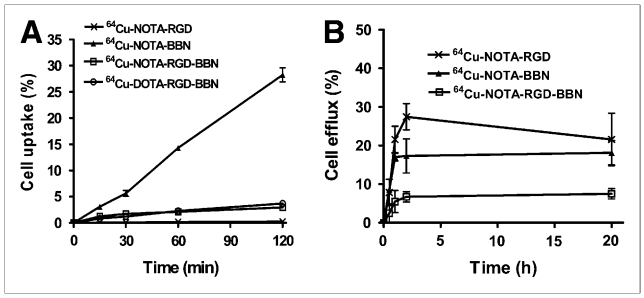

FIGURE 2. (A) Cell uptake assay of ^{64}Cu-NOTA-RGD, ^{64}Cu-NOTA-bombesin, ^{64}Cu-NOTA-RGD-bombesin, and ^{64}Cu-DOTA-RGD-bombesin on PC-3 cells (n = 3, mean ± SD). (B) Cell efflux assay of ^{64}Cu-NOTA-RGD, ^{64}Cu-NOTA-bombesin, and ^{64}Cu-NOTA-RGD-bombesin on PC-3 tumor cells (n = 3, mean ± SD). BBN = bombesin.

plateau, indicating that the cells maintained similar activity from a 2- to 10-h period. Although the efflux ratio was much lower for ^{64}Cu-NOTA-RGD-bombesin than for ^{64}Cu-NOTA-bombesin, cell retention was much higher for ^{64}Cu-NOTA-bombesin than for ^{64}Cu-NOTA-RGD-bombesin for up to 10 h (Supplemental Fig. 1E).

Small-Animal PET

All tumors were clearly visible after injection of the different tracers, with high contrast to contralateral background at all time points measured from 30 min to 20 h, except for ^{64}Cu-NOTA-RGD (Fig. 3). ^{64}Cu-NOTA-RGD showed relatively low tumor uptake in PC-3 tumors because of the low expression of integrin $\alpha_v\beta_3$ in PC-3 tumor tissue and the low affinity of monomeric RGD peptide with integrin receptor. Mice receiving ^{64}Cu-NOTA-bombesin or ^{64}Cu-NOTA-RGD plus ^{64}Cu-NOTA-RGD showed a predominantly intestinal accumulation of the activity. Prominent kidney uptake of ^{64}Cu-NOTA-RGD-bombesin and ^{64}Cu-DOTA-RGD-bombesin at early time points was observed, suggesting that the peptide heterodimer tracers are excreted mainly through the kidneys. The quantified tumor and major organ uptake of the tracers is depicted in Table 1, and the clearance curves and tumor-to-nontumor ratios are compared in Supplemental Figures 2 and 3. For ^{64}Cu-NOTA-RGD, ^{64}Cu-NOTA-bombesin, ^{64}Cu-NOTA-RGD plus ^{64}Cu-NOTA-bombesin, and ^{64}Cu-NOTA-RGD-bombesin, the tracers cleared rapidly from the blood, with less than 1 %ID/g remaining at 30 min after injection. ^{64}Cu-NOTA-RGD-bombesin showed slightly lower blood clearance than the other tracers, whereas ^{64}Cu-NOTA-bombesin cleared the most rapidly. The tumor uptake of ^{64}Cu-NOTA-RGD-bombesin was determined to be 3.06 ± 0.11, 2.78 ± 0.56, 2.21 ± 0.49, and 2.04 ± 0.35 %ID/g at 0.5, 1, 4, and 20 h after injection, respectively—significantly higher than all the other tracers tested ($P < 0.01$, $n = 4$/group, Table 1). Tumor uptake was about the same for ^{64}Cu-NOTA-RGD, ^{64}Cu-NOTA-bombesin, and ^{64}Cu-NOTA-RGD plus ^{64}Cu-NOTA-bombesin from 1 to 20 h after injection. ^{64}Cu-NOTA-RGD-bombesin showed higher kidney uptake than the other tracers at any time examined. ^{64}Cu-NOTA-RGD and ^{64}Cu-NOTA-RGD plus ^{64}Cu-NOTA-bombesin showed a similar clearance curve in the kidneys, whereas the kidney uptake of ^{64}Cu-NOTA-bombesin was the lowest at all time points. ^{64}Cu-NOTA-bombesin and ^{64}Cu-NOTA-RGD plus ^{64}Cu-NOTA-bombesin exhibited predominantly liver uptake, whereas uptake of ^{64}Cu-NOTA-RGD-bombesin and ^{64}Cu-NOTA-RGD in the liver was relatively low. The tumor-to-nontumor ratios of ^{64}Cu-NOTA-RGD-bombesin were significantly higher than those of the other tracers at 4 h after injection ($P < 0.05$, Supplemental Fig. 2), mostly because of the high tumor uptake of ^{64}Cu-

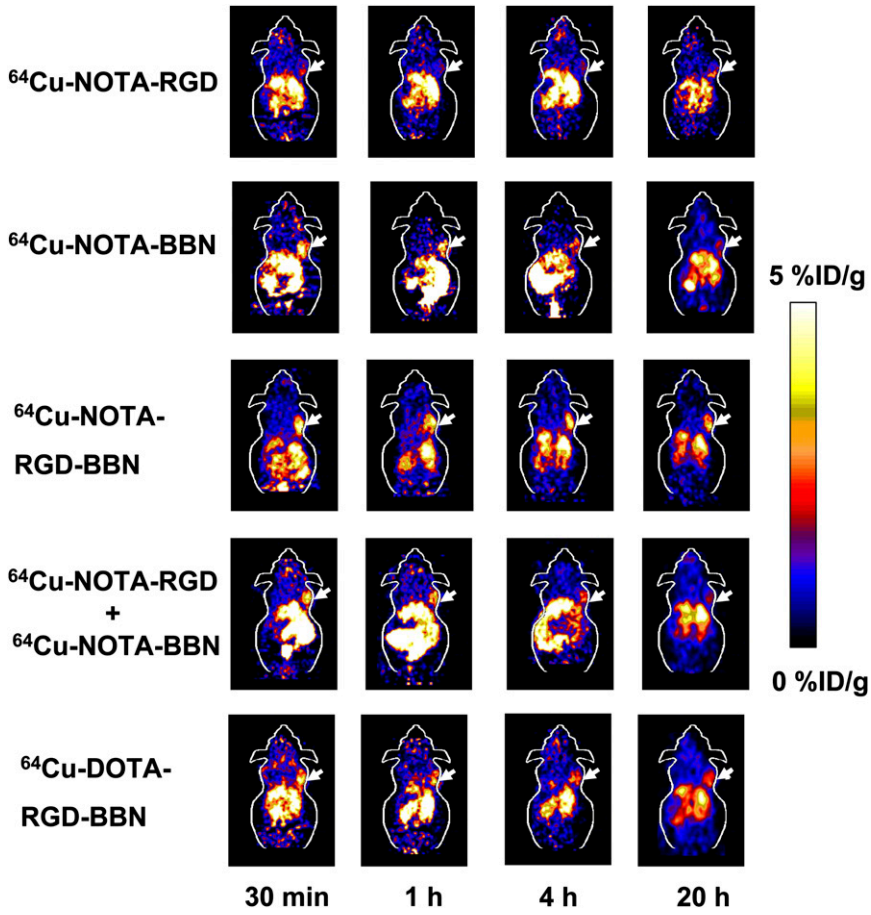

FIGURE 3. Decay-corrected whole-body coronal small-animal PET images of PC-3 tumor-bearing mice at 30 min, 1 h, 4 h, and 20 h after injection of approximately 5.5 MBq (150 μCi) of ^{64}Cu-NOTA-RGD, ^{64}Cu-NOTA-bombesin, ^{64}Cu-NOTA-RGD-bombesin, ^{64}Cu-NOTA-RGD plus ^{64}Cu-NOTA-bombesin, or ^{64}Cu-DOTA-RGD-bombesin. Images shown are static scans of a single mouse, which is representative of the 4 mice tested in each group. Arrows indicate presence of PC-3 tumors. BBN = bombesin.

TABLE 1. Small-Animal PET Data of ^{64}Cu-Labeled Tracers in PC-3 Mice

Tracer	Tissue or organ	30 min	1 h	4 h	20 h
^{64}Cu-NOTA-RGD	Blood	0.44 ± 0.15	0.43 ± 0.32	0.30 ± 0.11	0.34 ± 0.18
	Liver	2.86 ± 1.06	2.68 ± 1.15	2.15 ± 0.79	1.67 ± 0.69
	Kidney	3.37 ± 0.89	2.13 ± 0.85	1.43 ± 0.68	0.98 ± 0.48
	Tumor	1.01 ± 0.29	0.83 ± 0.24	0.66 ± 0.21	0.55 ± 0.32
^{64}Cu-NOTA-bombesin	Blood	0.74 ± 0.36	0.23 ± 0.11	0.19 ± 0.10	0.15 ± 0.05
	Liver	10.45 ± 2.27	8.85 ± 1.61	6.35 ± 0.57	4.20 ± 0.53
	Kidney	3.55 ± 1.17	1.50 ± 0.39	0.76 ± 0.45	0.50 ± 0.44
	Tumor	2.28 ± 0.35	1.25 ± 1.03	0.56 ± 0.40	0.44 ± 0.39
^{64}Cu-NOTA-RGD plus ^{64}Cu-NOTA-bombesin	Blood	0.79 ± 0.24	0.71 ± 0.23	0.31 ± 0.26	0.26 ± 0.18
	Liver	9.64 ± 4.15	6.74 ± 2.86	5.48 ± 0.84	3.24 ± 0.78
	Kidney	3.58 ± 0.98	1.83 ± 1.01	1.57 ± 0.87	0.84 ± 0.60
	Tumor	2.22 ± 0.41	1.27 ± 0.50	0.87 ± 0.35	0.54 ± 0.39
^{64}Cu-NOTA-RGD-bombesin	Blood	0.68 ± 0.03	0.66 ± 0.15	0.49 ± 0.07	0.50 ± 0.15
	Liver	3.46 ± 0.26	2.80 ± 1.15	1.83 ± 0.68	0.98 ± 0.40
	Kidney	4.09 ± 0.81	3.06 ± 0.25	2.30 ± 0.41	1.87 ± 0.41
	Tumor	3.06 ± 0.11	2.78 ± 0.56	2.21 ± 0.49	2.04 ± 0.35
^{64}Cu-DOTA-RGD-bombesin	Blood	1.15 ± 0.49	0.69 ± 0.24	0.45 ± 0.20	0.31 ± 0.13
	Liver	3.40 ± 1.42	3.05 ± 1.07	2.33 ± 0.88	1.74 ± 0.90
	Kidney	5.99 ± 1.61	3.40 ± 1.25	2.51 ± 0.47	1.64 ± 0.34
	Tumor	3.05 ± 0.56	1.87 ± 0.41	1.05 ± 0.49	0.97 ± 0.24

Injection dose was ~5.5 MBq (150 μCi) per mouse. Data are %ID/g ± SD (n = 4/group).

NOTA-RGD-bombesin. The pancreas could not be delineated on small-animal PET because of the limit of the spatial resolution.

The tumor and major organ uptake and tumor-to-nontumor ratios of ^{64}Cu-NOTA-RGD-bombesin and ^{64}Cu-DOTA-RGD-bombesin are directly compared in Supplemental Figure 3. For blood and kidneys, the 2 tracers showed almost identical clearance curves. The tumor uptake of ^{64}Cu-NOTA-RGD-bombesin was much higher than that of ^{64}Cu-DOTA-RGD-bombesin after 1 h after injection. For example, at 4 h after injection, the tumor uptake was 2.21 ± 0.49 %ID/g and 1.05 ± 0.49 %ID/g for ^{64}Cu-NOTA-RGD-bombesin and ^{64}Cu-DOTA-RGD-bombesin, respectively ($P < 0.05$, n = 4/group, Table 1). Liver uptake was similar for the 2 tracers at 30 min after injection, but liver uptake of ^{64}Cu-NOTA-RGD-bombesin became gradually lower than that of ^{64}Cu-DOTA-RGD-bombesin. Because of the similar normal-organ uptake and much higher tumor uptake of ^{64}Cu-NOTA-RGD-bombesin, the tumor-to-nontumor ratios of ^{64}Cu-NOTA-RGD-bombesin were all higher than those of ^{64}Cu-DOTA-RGD-bombesin after the 1-h time point ($P < 0.05$, n = 4/group).

The in vivo behaviors of ^{64}Cu-NOTA-RGD, ^{64}Cu-NOTA-bombesin, and ^{64}Cu-NOTA-RGD-bombesin were also tested in a murine 4T1 breast tumor model. The 4T1 tumor tissue expresses a moderate level of murine integrin β_3 but undetectable GRPR (data not shown). As shown in Figure 4A, ^{64}Cu-NOTA-bombesin had virtually no uptake in 4T1 tumors, whereas both ^{64}Cu-NOTA-RGD and ^{64}Cu-NOTA-RGD-bombesin showed clear tumor contrast due to the integrin $\alpha_v\beta_3$ recognition of RGD monomer and RGD-bombesin heterodimer in vivo, respectively. At the 2-h time point, tumor uptake of ^{64}Cu-NOTA-RGD, ^{64}Cu-NOTA-bombesin, and ^{64}Cu-NOTA-RGD-bombesin was 0.65 ± 0.07, 0.33 ± 0.18, and 1.88 ± 0.28 %ID/g, respectively (n = 3/group, Fig. 4B).

The in vivo integrin and GRPR dual-receptor binding property of ^{64}Cu-NOTA-RGD-bombesin was confirmed by several blocking studies (Fig. 4D). The tumor uptake of ^{64}Cu-NOTA-RGD-bombesin was only partially inhibited by either RGD (from 2.78 ± 0.56 %ID/g to 1.64 ± 0.77 %ID/g) or bombesin (from 2.78 ± 0.56 %ID/g to 0.76 ± 0.36 %ID/g). However, when ^{64}Cu-NOTA-RGD-bombesin was coadministered with both RGD and bombesin, the tumor uptake was almost totally blocked (0.54 ± 0.41 %ID/g) (Fig. 4C, n = 3/group).

Biodistribution Studies

The biodistribution of ^{64}Cu-NOTA-RGD-bombesin (370 kBq/mouse) was examined in normal BALB/c mice. The blocking experiments were also performed by coinjecting ^{64}Cu-NOTA-RGD-bombesin with a saturating dose of RGD, bombesin, or RGD plus bombesin and then sacrificing the mice at 1 h after injection (n = 4/group). As shown in Figure 5, the pancreas had predominant uptake of ^{64}Cu-NOTA-RGD-bombesin at 1 h after injection because of the high GRPR expression of this organ (*23*). In the presence of a blocking dose of bombesin or RGD plus bombesin, pancreatic uptake of the tracer decreased significantly from 7.03 ± 1.96 %ID/g to 2.08 ± 0.57 %ID/g (bombesin blocking) and 2.01 ± 0.18 %ID/g (RGD-plus-bombesin blocking), respectively ($P < 0.01$), indicating GRPR-

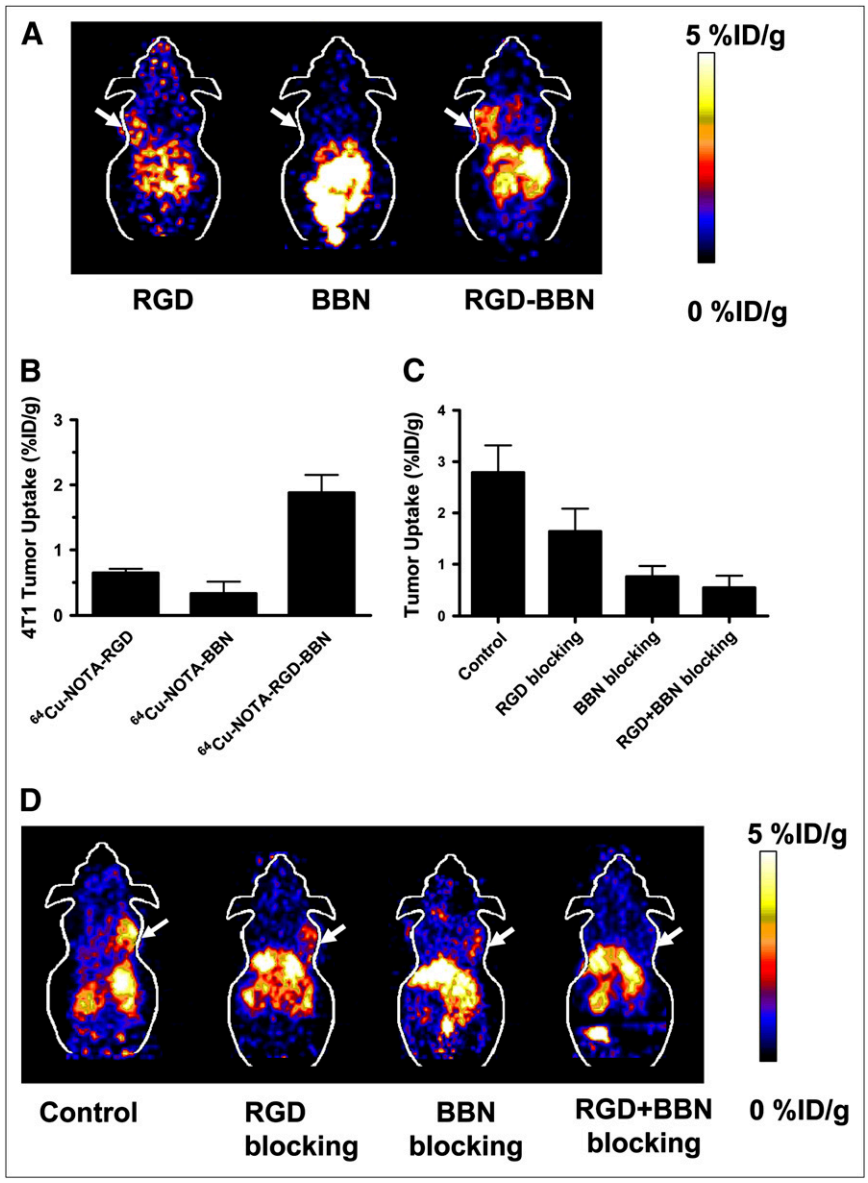

FIGURE 4. (A) Decay-corrected whole-body coronal small-animal PET images of 4T1 murine breast cancer–bearing mice at 2 h after injection of 3.7 MBq (100 μCi) of ^{64}Cu-NOTA-RGD, ^{64}Cu-NOTA-bombesin, or ^{64}Cu-NOTA-RGD-bombesin. Images shown are 5-min static scans of a single mouse, which is representative of the 3 mice tested in each group. Arrows indicate presence of 4T1 tumors. (B) Comparison of quantified tumor uptake of ^{64}Cu-NOTA-RGD, ^{64}Cu-NOTA-bombesin, and ^{64}Cu-NOTA-RGD-bombesin in 4T1 tumor-bearing mice. Regions of interest are shown as %ID/g ± SD (n = 3/group). (C) Comparison between uptake of ^{64}Cu-NOTA-RGD-bombesin in PC-3 tumor with or without preinjection of blocking doses of RGD, bombesin, or RGD plus bombesin. Regions of interest are shown as %ID/g ± SD (n = 3–4/group). (D) Decay-corrected whole-body coronal small-animal PET images of PC-3 tumor-bearing mice at 1 h after injection of approximately 5.5 MBq (150 μCi) of ^{64}Cu-NOTA-RGD-bombesin and in the presence of blocking dose of RGD, bombesin, or RGD plus bombesin (n = 3/group). BBN = bombesin.

specific targeting of ^{64}Cu-NOTA-RGD-bombesin in vivo. Blood uptake of ^{64}Cu-NOTA-RGD-bombesin decreased after coinjection of RGD or RGD plus bombesin, probably because the excess dose of RGD increased clearance of the tracer. Liver uptake was unaffected by blocking with bombesin or both RGD plus bombesin but slightly increased after blocking with RGD. Stomach and intestinal uptake of the tracer decreased after blocking with bombesin or RGD plus bombesin but slightly increased after blocking with RGD.

DISCUSSION

In this study, we evaluated the behaviors of ^{64}Cu-labeled RGD-bombesin heterodimer and explored its advantages over the monomeric counterparts. ^{64}Cu was chosen because of its favorable decay characteristics (half-life, 12.7 h; β^+, 17.8%; β^-, 38.4%), making it useful for both PET and internal radiotherapy. ^{64}Cu can be produced in high yield and at high specific activity on a small biomedical cyclotron and is labeled with biomolecules through macrocyclic chelators, which allow possible kit formulation and wide availability. More important, the longer half-life of ^{64}Cu among all the positron emitters allows imaging at late time points to acquire more in vivo information than is possible for ^{18}F (half-life, 109.7 min).

Both DOTA and NOTA can be used as bifunctional chelators for ^{64}Cu labeling. The ^{64}Cu-DOTA conjugates usually exhibit a high accumulation of liver radioactivity (*17,24*) because of the dissociation of ^{64}Cu in vivo from DOTA, followed by metabolism and transchelation to other proteins (*16,25,26*). NOTA is most commonly used for ^{68}Ga (half-life, 68 min) labeling because the rapid reaction kinetics of NOTA match the short half-life of ^{68}Ga. NOTA was also reported to be labeled with ^{64}Cu, with reduced liver accumulation (*15*). In the present study, we synthesized DOTA-RGD-bombesin and NOTA-RGD-bombesin

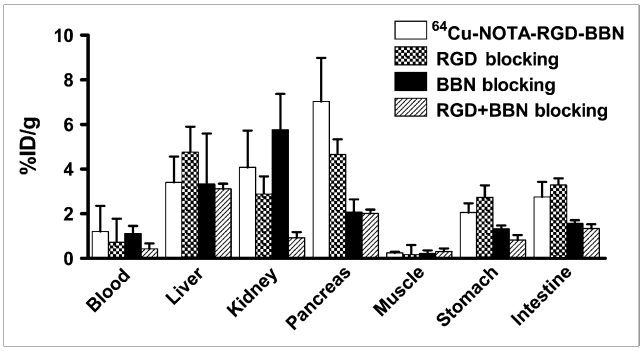

FIGURE 5. Biodistribution and blocking studies of ^{64}Cu-NOTA-RGD-bombesin (370 kBq/mouse) in normal BALB/c mice at 1 h after injection of tracer with or without blocking dose of RGD, bombesin, or RGD plus bombesin. Data are expressed as %ID/g ± SD (n = 4/group). BBN = bombesin.

and labeled both conjugates with ^{64}Cu. Compared with DOTA-RGD-bombesin, NOTA-RGD-bombesin can be more easily labeled with ^{64}Cu (Supplemental Fig. 1A). The direct in vivo comparison of ^{64}Cu-NOTA-RGD-bombesin and ^{64}Cu-DOTA-RGD-bombesin showed the former to have much higher tumor uptake and tumor-to-nontumor ratios and lower liver uptake than the latter. Several studies reported that cross-bridged chelators such as 1,4,8,11-tetraazabicyclo[6.6.2]hexadecane-4,11-diacetic acid (CB-TE2A) chelated ^{64}Cu more stably than did traditional chelators such as DOTA and 1,4,8,11-tetraazacyclo-dodecane-1,4,8,11-tetraacetic acid (*16,17,26*). The ^{64}Cu-labeled CB-TE2A chelated somatostatin receptor subtype 2 selective antagonist (sst_2-ANT) was recently reported as a promising PET tracer for somatostatin receptor–positive tumor imaging (*14*). Garrison et al. reported a ^{64}Cu-labeled bombesin analog using CB-TE2A as the chelator (*17*). ^{64}Cu-CB-TE2A-8-AOC-bombesin(7–14)NH_2 showed significant improvement in clearance because of its improved in vivo stability, compared with the DOTA conjugates. Most important, the liver uptake of the CB-TE2A conjugate was also significantly lower than that of the DOTA conjugates. Compared with ^{64}Cu-CB-TE2A-8-AOC-bombesin(7–14)NH_2, ^{64}Cu-NOTA-RGD-bombesin showed slightly higher liver uptake, but the tumor uptake of ^{64}Cu-NOTA-RGD-bombesin was also higher than that of ^{64}Cu-CB-TE2A-8-AOC-bombesin(7–14)NH_2, possibly because of the dual-receptor binding of the heterodimer in PC-3 tumor. Radiolabeling of CB-TE2A conjugates requires harsher reaction conditions than does radiolabeling of DOTA and NOTA conjugates (*17,27*). The high temperature and high pH required for CB-TE2A labeling may not be suitable for peptides such as RGD-bombesin. In contrast, the fast reaction kinetics of NOTA-conjugates would be more suitable for clinical translation.

The in vivo behaviors of the ^{64}Cu-labeled NOTA conjugates were compared in the PC-3 tumor model. Because of the high GRPR and low integrin $\alpha_v\beta_3$ expression of the PC-3 tumor, tumor uptake of ^{64}Cu-NOTA-RGD was low and the ^{64}Cu-NOTA-bombesin showed relatively high tumor contrast. However, high accumulation of radioactivity in the abdominal region, especially in the intestines, was observed in the mice receiving ^{64}Cu-NOTA-bombesin and other reported bombesin tracers (*8,17*), suggesting hepatobiliary excretion of ^{64}Cu-NOTA-bombesin. In contrast, ^{64}Cu-NOTA-RGD-bombesin showed much lower intestinal accumulation, and the tumor uptake of ^{64}Cu-NOTA-RGD-bombesin was also significantly higher than that of ^{64}Cu-NOTA-RGD, ^{64}Cu-NOTA-bombesin, and ^{64}Cu-NOTA-RGD plus ^{64}Cu-NOTA-RGD. The high lipophilicity of ^{64}Cu-NOTA-bombesin resulted in rapid hepatobiliary excretion, which led to a short circulation half-life for the tracer (Supplemental Fig. 2A) and thus insufficient time for the tracer to extravasate from the tumor blood vessels, diffuse in the extracellular space, and bind with GRPR expressed on the tumor cells. In contrast, ^{64}Cu-NOTA-RGD-bombesin had longer blood retention and predominantly renal clearance. Another major reason for the higher tumor uptake of ^{64}Cu-NOTA-RGD-bombesin than of ^{64}Cu-NOTA-bombesin is the dual GRPR- and integrin-targeting properties of the RGD-bombesin heterodimer (Fig. 4D). Although tumor uptake of RGD alone is low, binding of the RGD motif in the RGD-bombesin heterodimer molecule with integrins expressed on the tumor vasculature would significantly increase the local concentration of peptide in the tumor, facilitating the binding of bombesin with GRPR on tumor cells around the blood vessels. This may also explain why tumor uptake of ^{64}Cu-NOTA-RGD-bombesin was much higher than that of the coinjection of ^{64}Cu-NOTA-RGD plus ^{64}Cu-NOTA-bombesin, as was also found in the case of ^{18}F-FB-PEG_3-RGD-bombesin (*9*). The dual-receptor targeting of ^{64}Cu-NOTA-RGD-bombesin may also contribute to prolonged tumor retention of the tracer. For example, at 24 h after injection, tumor uptake of ^{64}Cu-NOTA-RGD-bombesin was 2.04 ± 0.35 %ID/g, which is significantly higher than that of the corresponding ^{64}Cu-NOTA-bombesin (0.44 ± 0.39 %ID/g). Tumor retention of ^{64}Cu-NOTA-RGD-bombesin was also higher than that of the ^{64}Cu-labeled NOTA conjugated bombesin tracers reported by Prasanphanich et al. (*15*). The prolonged tumor retention of ^{64}Cu-NOTA-RGD-bombesin, compared with that of ^{64}Cu-NOTA-bombesin, was consistent with the in vitro findings that the efflux ratio of ^{64}Cu-NOTA-RGD-bombesin was much lower than that of the bombesin tracer (Fig. 2B).

The PET images of mice that received ^{64}Cu-NOTA-RGD plus ^{64}Cu-NOTA-bombesin represented almost a merge of the images acquired after injection of ^{64}Cu-NOTA-RGD and ^{64}Cu-NOTA-bombesin alone (Fig. 3). For example, ^{64}Cu-NOTA-RGD showed clear kidney uptake and ^{64}Cu-NOTA-bombesin showed predominantly intestinal accumulation, whereas the coinjection of ^{64}Cu-NOTA-RGD and ^{64}Cu-NOTA-bombesin exhibited both renal and abdominal uptake (Fig. 3). The reduced liver and intestinal accumulation and increased tumor uptake of ^{64}Cu-NOTA-RGD-

bombesin, compared with ^{64}Cu-NOTA-RGD plus ^{64}Cu-NOTA-bombesin, clearly demonstrates that ^{64}Cu-NOTA-RGD-bombesin is superior to the sum of ^{64}Cu-NOTA-RGD and ^{64}Cu-NOTA-bombesin. The advantage of ^{64}Cu-NOTA-RGD-bombesin over ^{64}Cu-NOTA-RGD and ^{64}Cu-NOTA-bombesin was also confirmed in a 4T1 tumor model that is only integrin-positive. ^{64}Cu-NOTA-bombesin was unable to detect 4T1 tumor because of the lack of GRPR expression. In contrast, both ^{64}Cu-NOTA-RGD and ^{64}Cu-NOTA-RGD-bombesin showed tumor contrast (Figs. 4A and 4B). Uptake of ^{64}Cu-NOTA-RGD-bombesin was even higher than that of ^{64}Cu-NOTA-RGD in 4T1 tumor, possibly as a result of the improved in vivo kinetics and increased circulation retention of ^{64}Cu-NOTA-RGD-bombesin over ^{64}Cu-NOTA-RGD. Future studies may include the development of a peptide dimer containing a c(RGDyK) moiety and a scrambled bombesin sequence to see whether the control peptide dimer will have tumor uptake and in vivo kinetics similar to those of RGD-bombesin in a 4T1 tumor model.

^{64}Cu-NOTA-RGD-bombesin had blood and kidney clearance curves comparable to those of our previously reported ^{18}F-PEG$_3$-RGD-bombesin tracer (*10*) in the first hour after injection, but between 1 and 2 h, the ^{18}F tracer cleared more rapidly, possibly because of the higher hydrophilicity of ^{18}F-PEG$_3$-RGD-bombesin. The PC-3 tumor uptake of ^{18}F-PEG$_3$-RGD-bombesin was also significantly higher than that of ^{64}Cu-NOTA-RGD-bombesin at 30 min (6.35 ± 2.52 vs. 3.06 ± 0.11 %ID/g) and 1 h (4.41 ± 0.71 vs. 2.78 ± 0.56 %ID/g). Although we did not scan at 2 h with ^{64}Cu-NOTA-RGD-bombesin, we speculate that tumor uptake of ^{64}Cu-NOTA-RGD-bombesin would be comparable to that of ^{18}F-PEG$_3$-RGD-bombesin (2.47 ± 0.81 %ID/g) (*10*) at 2 h, because tumor uptake of ^{64}Cu-NOTA-RGD-bombesin was 2.78 ± 0.56 %ID/g and 2.21 ± 0.49 %ID/g at 1 and 4 h, respectively. Although liver uptake of ^{64}Cu-NOTA-RGD-bombesin was relatively low (<3.5 %ID/g at any time point tested), it was still higher than that of ^{18}F-PEG$_3$-RGD-bombesin. Taken together, ^{18}F-PEG$_3$-RGD-bombesin is better than ^{64}Cu-NOTA-RGD-bombesin for tumor imaging within 2 h after injection. However, because of the short half-life of ^{18}F, the absolute tumor signal of ^{18}F-PEG$_3$-RGD-bombesin was low after 2 h. In contrast, the plateau in tumor uptake of ^{64}Cu-NOTA-RGD-bombesin from 4 to 20 h allows a persistent imaging signal. More important, because of the decay characteristics of ^{64}Cu, the longer tumor retention of ^{64}Cu-NOTA-RGD-bombesin makes possible GRPR-positive tumor-targeted therapy. Recently, ^{90}Y- and ^{177}Lu-labeled bombesin analogs were extensively investigated for GRPR-positive tumor-targeted radiotherapy (*28–30*). The improved in vivo kinetics and enhanced tumor uptake of RGD-bombesin heterodimer over bombesin suggests promise for the application of RGD-bombesin to GRPR-targeted tumor radiotherapy.

Although we have demonstrated the advantages of ^{64}Cu-NOTA-RGD-bombesin over ^{64}Cu-NOTA-RGD and ^{64}Cu-NOTA-bombesin, we did not set other controls such as the RAD-bombesin heterodimer and RGD-scramble bombesin heterodimer. Comparing such control heterodimers with RGD-bombesin might provide more useful information about the enhanced tumor uptake and improved in vivo kinetics of the heterodimer strategy. Furthermore, design and synthesis of RGD-bombesin heterodimers with different linkers between the 2 motifs, or synthesis of RGD dimer-bombesin or RGD-bombesin dimer heterodimers, also deserves further investigation to see if the combination of homodimerization and heterodimerization would be of additional benefit.

CONCLUSION

This study has demonstrated the advantages of ^{64}Cu-NOTA-RGD-bombesin over ^{64}Cu-NOTA-RGD, ^{64}Cu-NOTA-bombesin, and ^{64}Cu-DOTA-RGD-bombesin for small-animal PET of GRPR-positive tumors in a nude mouse model. The favorable in vivo kinetics and enhanced tumor uptake of ^{64}Cu-NOTA-RGD-bombesin warrant its further investigation for GRPR-positive tumor imaging and possible radiotherapy. The synergistic effects of RGD-bombesin heterodimer observed in this study also encourage further investigations of other novel heterodimers for tumor targeting.

ACKNOWLEDGMENTS

This work was supported, in part, by the National Cancer Institute (NCI R01 120188, R01 CA119053, R21 CA121842, R21 CA102123, P50 CA114747, U54 CA119367, and R24 CA93862). We thank the cyclotron teams of the University of Wisconsin for ^{64}Cu production. Zhaofei Liu acknowledges the China Scholarship Council (CSC) for partial financial support during his study at Stanford University.

REFERENCES

1. Anastasi A, Erspamer V, Bucci M. Isolation and structure of bombesin and alytesin, 2 analogous active peptides from the skin of the European amphibians *Bombina* and *Alytes*. *Experientia.* 1971;27:166–167.
2. Cornelio DB, Roesler R, Schwartsmann G. Gastrin-releasing peptide receptor as a molecular target in experimental anticancer therapy. *Ann Oncol.* 2007; 18:1457–1466.
3. Smith CJ, Volkert WA, Hoffman TJ. Radiolabeled peptide conjugates for targeting of the bombesin receptor superfamily subtypes. *Nucl Med Biol.* 2005;32:733–740.
4. Santos-Cuevas CL, Ferro-Flores G, Arteaga de Murphy C, Pichardo-Romero PA. Targeted imaging of gastrin-releasing peptide receptors with ^{99m}Tc-EDDA/HYNIC-[Lys^3]-bombesin: biokinetics and dosimetry in women. *Nucl Med Commun.* 2008;29:741–747.
5. Garrison JC, Rold TL, Sieckman GL, et al. Evaluation of the pharmacokinetic effects of various linking group using the ^{111}In-DOTA-X-BBN(7-14)NH$_2$ structural paradigm in a prostate cancer model. *Bioconjug Chem.* 2008;19:1803–1812.
6. Chen X, Park R, Hou Y, et al. MicroPET and autoradiographic imaging of GRP receptor expression with ^{64}Cu-DOTA-[Lys^3]bombesin in human prostate adenocarcinoma xenografts. *J Nucl Med.* 2004;45:1390–1397.
7. Zhang X, Cai W, Cao F, et al. ^{18}F-labeled bombesin analogs for targeting GRP receptor-expressing prostate cancer. *J Nucl Med.* 2006;47:492–501.
8. Yang YS, Zhang X, Xiong Z, Chen X. Comparative in vitro and in vivo evaluation of two ^{64}Cu-labeled bombesin analogs in a mouse model of human prostate adenocarcinoma. *Nucl Med Biol.* 2006;33:371–380.

9. Li ZB, Wu Z, Chen K, Ryu EK, Chen X. ^{18}F-labeled BBN-RGD heterodimer for prostate cancer imaging. *J Nucl Med.* 2008;49:453–461.
10. Liu Z, Yan Y, Chin FT, Wang F, Chen X. Dual integrin and gastrin-releasing peptide receptor targeted tumor imaging using ^{18}F-labeled PEGylated RGD-bombesin heterodimer ^{18}F-FB-PEG$_3$-Glu-RGD-BBN. *J Med Chem.* 2009;52: 425–432.
11. Cai W, Wu Y, Chen K, Cao Q, Tice DA, Chen X. In vitro and in vivo characterization of ^{64}Cu-labeled Abegrin, a humanized monoclonal antibody against integrin αvβ3. *Cancer Res.* 2006;66:9673–9681.
12. McCarthy DW, Shefer RE, Klinkowstein RE, et al. Efficient production of high specific activity ^{64}Cu using a biomedical cyclotron. *Nucl Med Biol.* 1997;24: 35–43.
13. Blower PJ, Lewis JS, Zweit J. Copper radionuclides and radiopharmaceuticals in nuclear medicine. *Nucl Med Biol.* 1996;23:957–980.
14. Wadas TJ, Eiblmaier M, Zheleznyak A, et al. Preparation and biological evaluation of ^{64}Cu-CB-TE2A-sst2-ANT, a somatostatin antagonist for PET imaging of somatostatin receptor-positive tumors. *J Nucl Med.* 2008;49:1819–1827.
15. Prasanphanich AF, Nanda PK, Rold TL, et al. [^{64}Cu-NOTA-8-Aoc-BBN(7-14)NH_2] targeting vector for positron-emission tomography imaging of gastrin-releasing peptide receptor-expressing tissues. *Proc Natl Acad Sci USA.* 2007; 104:12462–12467.
16. Boswell CA, Sun X, Niu W, et al. Comparative in vivo stability of copper-64-labeled cross-bridged and conventional tetraazamacrocyclic complexes. *J Med Chem.* 2004;47:1465–1474.
17. Garrison JC, Rold TL, Sieckman GL, et al. In vivo evaluation and small-animal PET/CT of a prostate cancer mouse model using ^{64}Cu bombesin analogs: side-by-side comparison of the CB-TE2A and DOTA chelation systems. *J Nucl Med.* 2007;48:1327–1337.
18. Li ZB, Chen K, Chen X. ^{68}Ga-labeled multimeric RGD peptides for microPET imaging of integrin αvβ3 expression. *Eur J Nucl Med Mol Imaging.* 2008;35: 1100–1108.
19. Wu Y, Zhang X, Xiong Z, et al. MicroPET imaging of glioma integrin αvβ3 expression using ^{64}Cu-labeled tetrameric RGD peptide. *J Nucl Med.* 2005;46: 1707–1718.
20. Liu Z, Niu G, Shi J, et al. ^{68}Ga-labeled cyclic RGD dimers with Gly_3 and PEG_4 linkers: promising agents for tumor integrin αvβ3 PET imaging. *Eur J Nucl Med Mol Imaging.* 2009;36:947–957.
21. Chen X, Park R, Shahinian AH, Bading JR, Conti PS. Pharmacokinetics and tumor retention of ^{125}I-labeled RGD peptide are improved by PEGylation. *Nucl Med Biol.* 2004;31:11–19.
22. Liu Z, Yu Z, He W, Ma S, Sun L, Wang F. In-vitro internalization and in-vivo tumor uptake of anti-EGFR monoclonal antibody LA22 in A549 lung cancer cells and animal model. *Cancer Biother Radiopharm.* 2009;24;15–24.
23. Hoffman TJ, Gali H, Smith CJ, et al. Novel series of ^{111}In-labeled bombesin analogs as potential radiopharmaceuticals for specific targeting of gastrin-releasing peptide receptors expressed on human prostate cancer cells. *J Nucl Med.* 2003;44:823–831.
24. Biddlecombe GB, Rogers BE, de Visser M, et al. Molecular imaging of gastrin-releasing peptide receptor-positive tumors in mice using ^{64}Cu- and ^{86}Y-DOTA-(Pro^1,Tyr^4)-bombesin(1-14). *Bioconjug Chem.* 2007;18:724–730.
25. Wadas TJ, Wong EH, Weisman GR, Anderson CJ. Copper chelation chemistry and its role in copper radiopharmaceuticals. *Curr Pharm Des.* 2007;13:3–16.
26. Sprague JE, Peng Y, Sun X, et al. Preparation and biological evaluation of copper-64-labeled tyr^3-octreotate using a cross-bridged macrocyclic chelator. *Clin Cancer Res.* 2004;10:8674–8682.
27. Eiblmaier M, Meyer LA, Watson MA, Fracasso PM, Pike LJ, Anderson CJ. Correlating EGFR expression with receptor-binding properties and internalization of ^{64}Cu-DOTA-cetuximab in 5 cervical cancer cell lines. *J Nucl Med.* 2008;49:1472–1479.
28. Panigone S, Nunn AD. Lutetium-177-labeled gastrin releasing peptide receptor binding analogs: a novel approach to radionuclide therapy. *Q J Nucl Med Mol Imaging.* 2006;50:310–321.
29. Lantry LE, Cappelletti E, Maddalena ME, et al. ^{177}Lu-AMBA: synthesis and characterization of a selective ^{177}Lu-labeled GRP-R agonist for systemic radiotherapy of prostate cancer. *J Nucl Med.* 2006;47:1144–1152.
30. Chen J, Linder KE, Cagnolini A, et al. Synthesis, stabilization and formulation of [^{177}Lu]Lu-AMBA, a systemic radiotherapeutic agent for gastrin releasing peptide receptor positive tumors. *Appl Radiat Isot.* 2008;66:497–505.